BIOCHEMISTRY
including biophysical chemistry & molecular biology

Article

pubs.acs.org/biochemistry

Crystal Structure of a Membrane Stomatin-Specific Protease in Complex with a Substrate Peptide

Hideshi Yokoyama,*[,†] Naoto Takizawa,[†] Daisuke Kobayashi,[†] Ikuo Matsui,[‡] and Satoshi Fujii[†]

[†]School of Pharmaceutical Sciences, University of Shizuoka, Shizuoka 422-8526, Japan

[‡]Biomedical Research Institute, National Institute of Advanced Industrial Science and Technology (AIST), Tsukuba 305-8566, Japan

Supporting Information

ABSTRACT: Membrane-bound proteases are involved in various regulatory functions. A previous report indicated that the N-terminal region of PH1510p (1510-N) from the hyperthermophilic archaeon *Pyrococcus horikoshii* is a serine protease with a catalytic Ser-Lys dyad (Ser97 and Lys138) and specifically cleaves the C-terminal hydrophobic region of the p-stomatin PH1511p. In humans, an absence of stomatin is associated with a form of hemolytic anemia known as hereditary stomatocytosis. Here, the crystal structure of 1510-N K138A in complex with a peptide substrate was determined at 2.25 Å resolution. In the structure, a 1510-N dimer binds to one peptide. The six central residues (VIVLML) of the peptide are hydrophobic and in a pseudopalindromic structure and therefore favorably fit into the hydrophobic active tunnel of the 1510-N dimer, although 1510-N degrades the substrate at only one point. A comparison with unliganded 1510-N K138A revealed that the binding of the substrate causes a large rotational and translational displacement between protomers and produces a tunnel suitable for binding the peptide. When the peptide binds, the flexible L2 loop of one protomer forms β-strands, whereas that of the other protomer remains in a loop form, indicating that one protomer binds to the peptide more tightly than the other protomer. The Ala138 residues of the two protomers are located very close together (the distance between the two Cβ atoms is 3.6 Å). Thus, in wild-type 1510-N, the close positioning of the catalytic Ser97 and Lys138 residues may be induced by electrostatic repulsion of the two Lys138 side chains of the protomers.

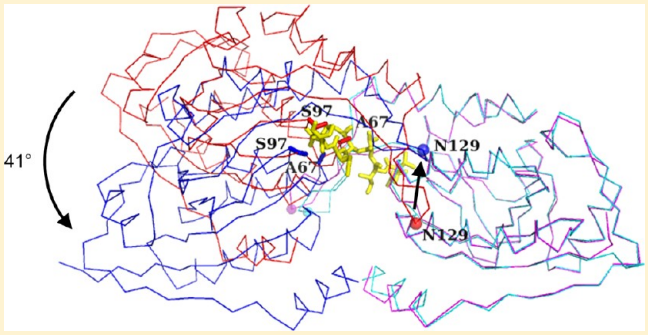

Membrane-bound proteases play several important roles in protein quality control and regulation. Mitochondrial membranes possess quality control systems that remove nonassembled polypeptides and prevent the possibly deleterious accumulation of these proteins in the membrane.[1] The regulatory system is also mediated by membrane-embedded proteases specific for different substrates. Several transcription factors are synthesized as membrane proteins and activated upon the specific proteolytic cleavage of solvent-exposed fragments that subsequently enter the nucleus.[2,3] Elucidation of these membrane proteases will lead to an improved understanding of crucial biological processes and disease.

Stomatin, prohibitin, flotillin, and HflK/C (SPFH) domain proteins are found in lipid raft microdomains in various cellular membranes.[4,5] Stomatin was first identified in human erythrocytes. The absence of the protein is associated with a form of hemolytic anemia known as hereditary stomatocytosis.[6] Stomatin is also widely expressed in various tissues and cell lines and localized in detergent-resistant membrane domains.[7,8] It is organized into higher-order homo-oligomeric complexes of ~300 kDa, comprised of 9−12-mers.[9] Stomatin interacts with and modulates the activity of acid-sensing ion channels (ASICs)[10,11] and glucose transporter type 1 (GLUT-1).[12,13] Human stomatin has also been identified as a major component of vesicles produced by red cells.[14] Recently, it was reported that stomatin is widely expressed in the central nervous system (CNS) of rats and involved in various cellular events of neurons in the CNS under physiological conditions.[15]

Stomatin-like proteins are found in almost all species of eukaryotes, bacteria, and archaea.[4] In both archaeal and bacterial species, p-stomatin (prokaryotic stomatin) and STOPP (stomatin operon partner protein) genes probably form an operon.[16] STOPP is also known as nfeD (nodulation formation efficiency D). In the hyperthermophilic archaeon *Pyrococcus horikoshii*, there are two sets of NfeD/stomatin gene pairs, PH1510/PH1511 and PH0471/PH0470. The N-terminal region of NfeD PH1510p (residues 16−236, 1510-N) is a serine protease with a catalytic Ser-Lys dyad (Ser97 and Lys138) and specifically cleaves the C-terminal hydrophobic region of the p-stomatin PH1511p.[17] In proteases with the Ser-Lys catalytic dyad, a lysine side chain acts as the general base to increase the nucleophilicity of the catalytic serine, allowing the serine to attack the carbonyl group of the amide bond within the protein substrate, and afterward, the oxyanion intermediate

Received: January 23, 2012
Revised: April 3, 2012
Published: April 4, 2012

   dx.doi.org/10.1021/bi300098k | *Biochemistry* 2012, 51, 3872−3880

is formed.[18,19] The crystal structure of wild-type 1510-N is similar to that of the ClpP protease in *Escherichia coli*, and each active site around Ser97 is in a hydrophobic environment suitable for hydrophobic substrates.[20] The C-terminal region of NfeD PH0471p shows a compact five-β-strand barrel, which is structurally similar to the OB fold (oligosaccharide/oligonucleotide-binding fold).[21] In the crystal structure of the p-stomatin PH1511p, the SPFH domain forms a stable trimer, and three C-terminal α-helical domains extend from the apexes of the triangle.[22] Another p-stomatin, PH0470p, also has the SPFH domain structure.[23] Linkages between proteases and other SPFH proteins are observed as well. The *E. coli* SPFH proteins, HflK and HflC, form a complex with FtsH, a protease involved in protein quality control, and regulate FtsH activity.[24] Another *E. coli* SPFH protein, YbbK, which was renamed QmcA, forms an oligomer and interacts with FtsH.[25]

It is not known precisely how these proteases recognize SPFH proteins. To prevent the proteolytic cleavage of 1510-N during crystallization, we made the catalytically inactive mutants S97A and K138A, both of which show no activity.[17,20] Here we report the crystal structure of the K138A mutant of 1510-N in complex with a 10-amino acid peptide of the stomatin PH1511p. The structure shows that a single peptide could be bound to the 1510-N dimer via a specific mode of binding through an unequal structural change between the two protomers.

EXPERIMENTAL PROCEDURES

Protein Preparation and Crystallization. The K138A mutant of 1510-N was prepared mostly as described previously.[17,26] In the final stage, the protein was purified with a HiTrap Q HP anion-exchange column in an AKTAprime plus system (GE Healthcare) using a buffer containing 50 mM Tris-HCl (pH 8.5) and then eluted with a linear gradient from 0 to 1 M NaCl. The purified protein was mixed with the 10-amino acid synthetic peptide NVIVLMLPME at a molar ratio of 1:10. The protein/peptide solution contained 9.1 mg/mL 1510-N K138A and 4.2 mg/mL peptide in a buffer containing 30 mM Tris-HCl (pH8.5), 0.1 M NaCl, and 8.4% (v/v) dimethyl sulfoxide. Crystallization drops were prepared by mixing equal volumes of the protein/peptide and reservoir solutions. Crystals were grown at 20 °C with the hanging-drop vapor diffusion method, using a reservoir solution containing 1.0 M imidazole (pH7.5). Cubic crystals grew to an approximate size of 0.20 mm per side.

Data Collection, Structure Determination, and Refinement. A crystal was cryoprotected in a solution containing 1.5 M imidazole (pH 7.5), 30% (v/v) glycerol, 25 mM Tris-HCl (pH8.5), and 0.15 M NaCl and flash-frozen at 95 K. X-ray diffraction data were collected on beamline NW12A of the Photon Factory in KEK (Tsukuba, Japan) with a Quantum 210r CCD detector and processed and scaled with HKL2000.[27]

The structure was determined by the molecular replacement method with MOLREP[28] in the CCP4 suite.[29] Unliganded 1510-N K138A (PDB entry 3bpp) was used as the initial model with part of the L2 region (residues 125−134) removed. After rigid-body refinement, the model was subjected to several cycles of crystallographic refinement with REFMAC5,[30] followed by manual model building and fitting with COOT.[31] Noncrystallographic symmetry (NCS) restraints were applied during the refinement and liberated during the final stage of refinement. Also in the final stage, TLS-restrained refinement was conducted with REFMAC5.[32] Interface areas were calculated with Protein interfaces, surfaces, and assemblies service PISA at the European Bioinformatics Institute (http://www.ebi.ac.uk/pdbe/prot_int/pistart.html), authored by E. Krissinel and K. Henrick. The least-squares fitting between two structures was performed with LSQKAB in the CCP4 suite. All figures were produced with PyMOL (http://www.pymol.org/).

RESULTS

Structure Determination. The K138A mutant of 1510-N was prepared as described previously.[26] The 1510-N protease specifically cleaves the middle of the C-terminal hydrophobic region of the p-stomatin PH1511p between residues 238 and 239 (^{234}NVIVL↓MLPME^{243}, where the arrow indicates the cleaved point).[17] Therefore, 1510-N K138A was mixed with a 10-amino acid synthetic peptide containing the sequence of PH1511p (^{234}NVIVLMLPME^{243}) and then crystallized. The crystal structure of 1510-N K138A in complex with the peptide substrate was determined at 2.25 Å resolution with the molecular replacement method (Table 1). The structure contains a 1510-N dimer and one substrate peptide per asymmetric unit. The refined model contains residues 19−237 in chains A and B of 1510-N K138A, residues 234−241 of PH1511p, and 172 solvent molecules. The Leu237 residues in

Table 1. Data Collection and Refinement Statistics

Data Collection	
space group	$P4_32_12$
cell dimensions (Å)	a = 111.5, c = 91.8
wavelength (Å)	1.0000
resolution range (Å)	20−2.25 (2.33−2.25)[a]
$R_{merge}(I)$[b]	0.054 (0.341)[a]
average $I/\sigma I$	67.9 (9.8)[a]
no. of unique reflections	27554
redundancy	10.6
completeness (%)	98.7 (100)[a]
Refinement	
resolution range (Å)	19.74−2.25
no. of reflections used	24628
completeness (%)	98.2
R_{work}[c]/R_{free}[d]	0.212/0.248
no. of atoms	
protein	3374
peptide	61
solvent	172
average B factor (Å^2)	
protein	52.4
peptide	68.9
solvent	40.5
root-mean-square deviation	
bond lengths (Å)	0.013
bond angles (deg)	1.338
Ramachandran plot[e] (%)	
favored region	96.6
allowed region	3.4
outlier region	0

[a]Values in parentheses are for the highest-resolution shell. [b]$R_{merge}(I) = \sum|I - \langle I\rangle|/\sum I$, where I is the observed diffraction intensity. [c]$R = \sum|F_o - F_c|/\sum F_o$, where F_o and F_c are observed and calculated structure factor amplitudes, respectively. [d]R_{free} is an R value for 10% of the reflections chosen randomly and omitted from the refinement. [e]Values for proteins and the peptide were calculated with RAMPAGE.[33]

dx.doi.org/10.1021/bi300098k | *Biochemistry* 2012, 51, 3872−3880

chains A and B correspond to the residues derived from the expression vector. The $F_o - F_c$ electron densities corresponding to the peptide are shown in Figure S1A of the Supporting Information. The densities between Asn234 and Leu238 are clear and continuous, whereas those between Met239 and Pro241 are low. The average B factor of all protein atoms is relatively high [52.4 Å^2 (Table 1)]. In particular, the L2 loops composed of residues 121−139 have high average B factors of 71.6 Å^2 (chain A) and 77.2 Å^2 (chain B). The electron densities of the L2 loop (chain A) are not good but continuous (Figure S1B of the Supporting Information). According to the stereochemistry of the protein and peptide model evaluated with RAMPAGE,[33] no residues are located in the outlier region (Table 1).

Overall Structure. The overall structure of 1510-N K138A in complex with a substrate peptide is shown in Figure 1. The dimer is approximately 80 Å in length, 35 Å in width, and 40 Å in height. The 1510-N homodimer binds to a peptide. The two long L2 loops of the dimer cover the peptide. A noncrystallographic pseudo-2-fold axis relating each protomer of 1510-N runs perpendicular to the plane in Figure 1A at its center. Both of the catalytic Ser97 residues of the 1510-N dimer are located around the N- and C-termini of the peptide (Figure 1A,B). The two catalytic Ala138 residues that replaced Lys are located close together as discussed later. The dimer constitutes a peptide-binding tunnel as shown in Figure 1C. The top side of the tunnel is rich in hydrophobic residues as shown in white, suitable for a hydrophobic substrate, whereas the bottom side contains the salt bridges between Arg66 and Asp68 as described below. Another large space is observed beneath the peptide-binding hole. The lower face of the C-terminal helices of 1510-N contains hydrophobic residues, composed of Phe226, Leu230, Tyr233, and Ile234, probably facing a cell membrane (Figure 1C).

Interaction with the Substrate. Figure 2 shows the interaction of 1510-N K138A with the peptide. The view is almost the opposite of that in Figure 1A. The main chain atoms of the peptide residues Asn234, Val235, Ile236, and Val237 interact with the main chain atoms of Ala119, Arg121, Ile123, Gly65, and Ala67 of chain A in pale colors (Figure 2A). Ala119, Arg121, and Ile123 are located at the base of the L2 loop, and Gly65 and Ala67 are located at the L1 loop, which is also known as a conserved TPGG motif.[16] The catalytic Ser97 Oγ atom is hydrogen-bonded to the Asn234 O atom of the peptide. Almost all the main chain nitrogen and carboxyl oxygen atoms of the Asn234−Val237 peptide are hydrogen-bonded to the L1 and L2 residues in a parallel β-sheet manner.

Among the peptide residues, Leu238, Met239, Leu240, and Pro241, however, the Ala67 N atom of chain B is hydrogen-bonded to the Leu238 O atom, and the Ile123 N atom of chain B is hydrogen-bonded to the Met239 O atom. The Ser97 Oγ atom of chain B is also hydrogen-bonded to the Leu240 O atom, and the Asp168 Oδ1 atom is hydrogen-bonded to the Pro241 O atom. Thus, the main chain atoms of the Leu238−Pro241 peptide have fewer hydrogen bonds in chain B than those of the Asn234−Val237 peptide in chain A. Meanwhile, the interface areas between the peptide and chain A (513 Å^2) and between the peptide and chain B (533 Å^2) are almost the same. The pseudo-2-fold axis running between chains A and B of 1510-N K138A runs perpendicular to the plane in Figure 2A at its center and also runs through the bond between Val237 and Leu238 of the peptide.

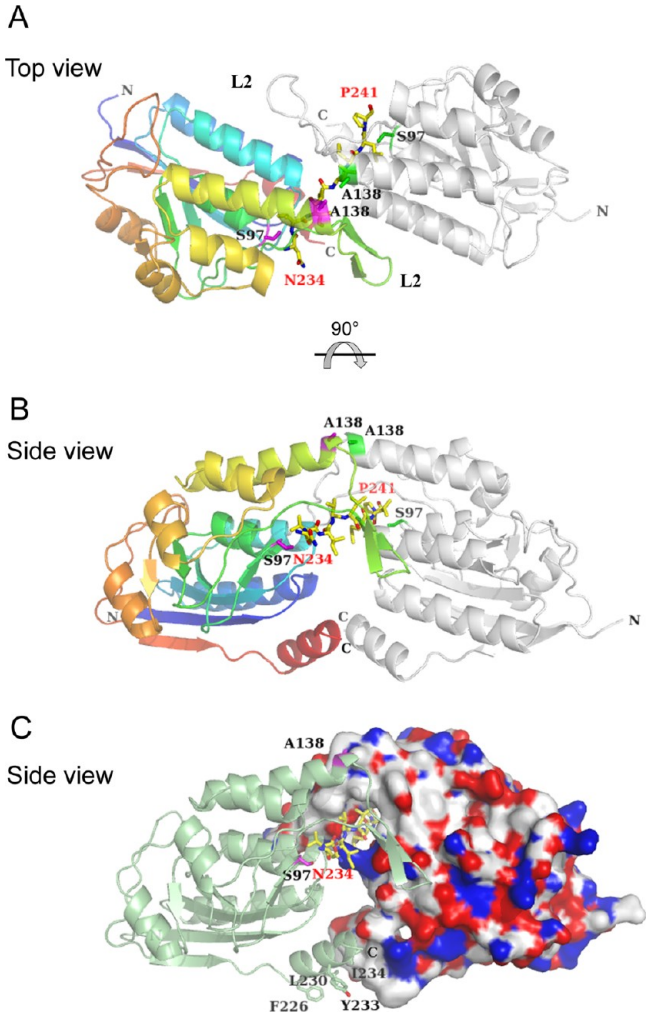

Figure 1. Overall structure of the 1510-N K138A dimer in complex with a peptide substrate. (A) Top view shown as a ribbon. One monomer (chain A) of 1510-N K138A is represented by a rainbow of colors, from purple at the N-terminus to red at the C-terminus. N and C denote the N- and C-termini, respectively. The other monomer (chain B) of 1510-N K138A is colored gray. The peptide is shown as a stick model, and Asn234 and Pro241 are labeled in red. The catalytic Ser97 and Ala138 (replaced Lys) residues in chain A are shown as magenta sticks, while those in chain B are shown as green sticks. (B) Side view. (C) Chain A of 1510-N K138A represented as a green ribbon, chain B as a surface model, and the peptide as a stick model. In chain B, negatively charged residues (Asp and Glu) are colored red and positively charged residues (Lys, Arg, and His) blue. The catalytic Ser97 and A138 residues of chain A are represented as magenta sticks. The residues located at the bottom of the C-terminal helix of chain A are shown as sticks. The view is almost the same as in panel B.

As shown in Figure 2B, the bottom of the peptide-binding site, which is located at the top site of Figure 1C, is rich in hydrophobic residues. The hydrophobic peptide residues, Val235, Ile236, Val237, Leu238, Met239, Leu240, and Pro241, are suitable for the binding pocket composed of Tyr101, Ieu123, Leu124, Tyr126, Ile132, Ile139, and Phe143, many of which are located in the L2 loop. As shown in Figure 2C, the side chain of Arg66 of chain A forms a salt bridge with that of Asp68 of chain B. Also, the side chain of Asp68 of chain A forms a salt bridge with that of Arg66 of chain B. The salt bridges located at the bottom site of the peptide-binding hole (Figure 1C) lock the peptide in the binding site. Around the N-

dx.doi.org/10.1021/bi300098k | Biochemistry 2012, 51, 3872−3880

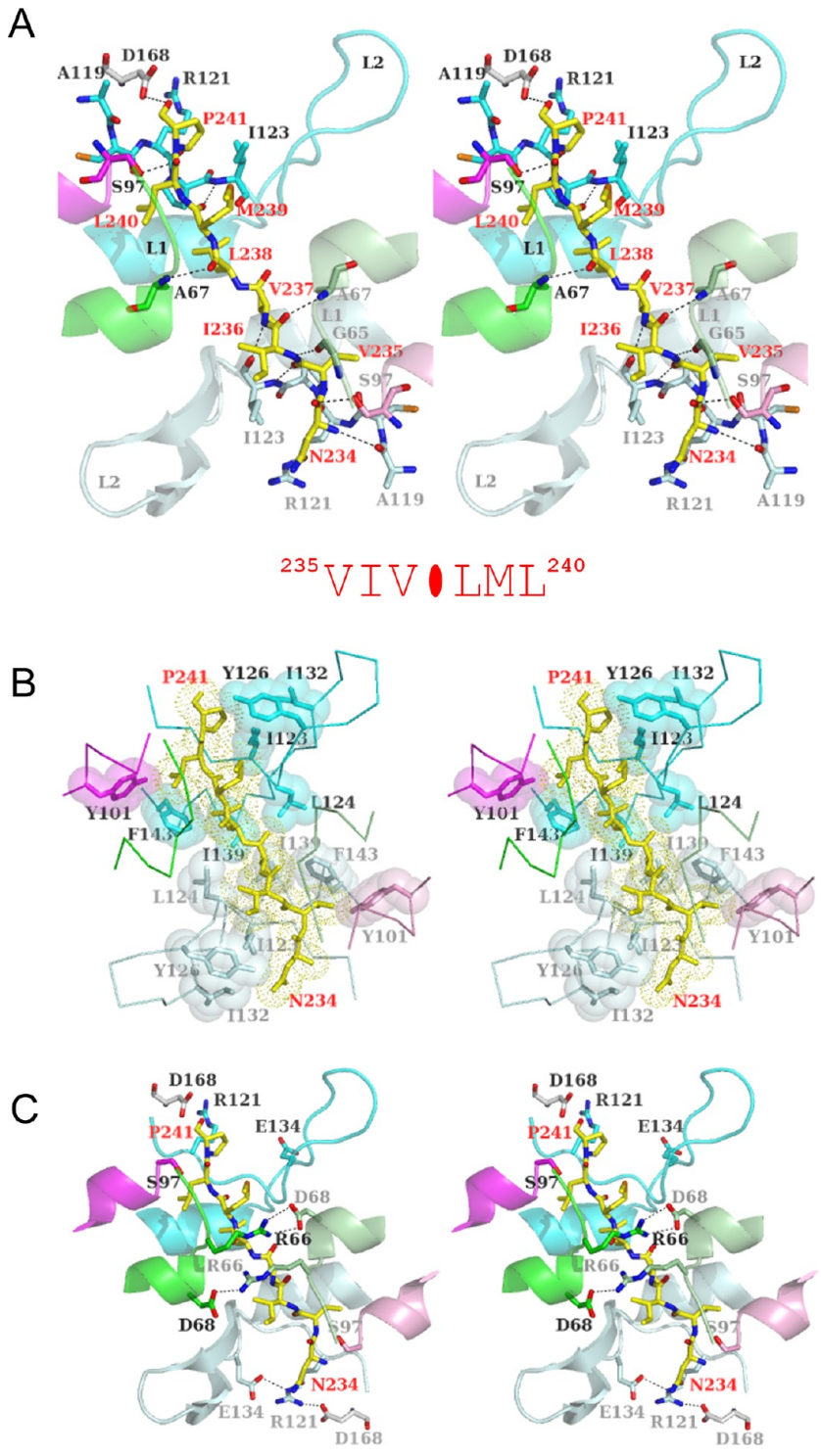

Figure 2. Stereo representation of the interaction between the peptide substrate and 1510-N K138A. The view is rotated 180° along the vertical axis on the plane in Figure 1A. The peptide is represented as yellow sticks. The L1 loop (residues 64−71), catalytic S97-containing residues 97−102, and the L2 loop (residues 119−144) in chain A (bottom right) are colored pale green, pink, and pale cyan, respectively. Those in chain B (top left) are colored green, magenta, and cyan, respectively. The residues of chain A, chain B, and the peptide are labeled in gray, black, and red, respectively. (A) Hydrogen bonds between the peptide and 1510-N K138A. At the bottom, the pseudopalindromic residues of the peptide are shown with red letters and a filled ellipsoid showing a pseudo-2-fold axis. (B) Hydrophobic interaction between the peptide and 1510-N K138A. Hydrophobic side chains of 1510-N K138A are shown as sticks and spheres, and the peptide is shown as sticks and dots. (C) Salt bridges formed near the peptide. Each view of panels A−C is almost the same.

terminal residue of the peptide, side chains of Asp168, Arg121, and Glu134 of chain A form salt bridges, which lock the peptide laterally. In chain B, no such salt bridges are observed, and thus, the exit of the C-terminal peptide is open. A previous report[17] indicated that the D168A mutant of 1510-N shows a low level of protease activity (3.2%) compared to the wild type (WT). Asp168 is important for forming salt bridges and interacting with the peptide.

dx.doi.org/10.1021/bi300098k | *Biochemistry* 2012, 51, 3872−3880

Comparison between Liganded and Unliganded Structures. The structures of the K138A mutant[26] and WT[20] 1510-N were determined previously. The two structures do not contain a substrate peptide and therefore correspond to unliganded forms. The liganded structure is similar to that of one dimer (type 2 as described in Table S1 of the Supporting Information) of the unliganded structure. Figure 3A shows the superposition of one protomer (chain A) of liganded and unliganded 1510-N K138A. Because the spatial positions of the L2 loop and C-terminal residues 223−235 deviate more between chains A and B than those of the other regions, residues 24−120 and 139−222 of chain A of liganded 1510-N K138A are fitted to those of the unliganded form, resulting in a low root-mean-square deviation (rmsd) of 0.33 Å. If residues 20−235 of chain A are all superposed, the rmsd is 1.11 Å. These results indicate that the core structure is nearly identical between liganded and unliganded monomers, whereas the L2 loop corresponding to residues 121−139 and C-terminal residues 223−235 are different. At the tip of the L2 loop, the Cα atom of Asn129 in chain A was found to be 3.6 Å closer to the center of the 1510-N dimer in the liganded monomer than in the unliganded monomer (Figure 3A). In the case of the superposition of chain B, the Cα atom of Asn129 was 3.7 Å closer to the center of the 1510-N dimer in the liganded monomer than in the unliganded monomer. The catalytic A138 Cβ atom is also relocated 13.4 Å from the unliganded monomer as shown with a black arrow (Figure 3A).

Dimer formation differs greatly between the liganded and unliganded structures. If one monomer is superposed, the liganded chain B shows a 41° counterclockwise rigid-body rotation relative to the other monomer of the unliganded form (Figure 3B), and the Cα atom of Asn129, which is located at the tip of the L2 loop, is positioned 10.5 Å upward from the unliganded monomer. In the superposed structures, the peptide ligand lies in the space occupied by residues Ala67 and Ser97 of the unliganded monomer (Figure 3B).

Comparison of Two Protomers. Figure 3C shows the superposition of two protomers of the liganded structure. Residues 24−120 and 139−222 of chain B of liganded 1510-N K138A are superposed with those of chain A, resulting in a low rmsd of 0.21 Å. If residues 19−237 are all superposed, the rmsd is 1.00 Å. Compared with chain B, the Asn129 Cα atom of chain A is 2.4 Å closer to the center of the 1510-N dimer, and the C-terminus is 4.7 Å closer to the center of the 1510-N dimer. As described in Figure S1A of the Supporting Information, the N-terminal portion of the peptide of PH1511p (residues Asn234−Val237) located around chain A shows clear and continuous electron densities and an average *B* factor of 61.3 Å^2. On the other hand, the C-terminal portion of the peptide of PH1511p (residues Leu238−Pro241) located around chain B shows low densities and an average *B* factor of 76.5 Å^2. These results indicate that chain A interacts more stably with the peptide than chain B. Also, the L2 loop of chain A forms antiparallel β-strands, whereas that of chain B forms only a loop structure. The structural heterogeneity between chains A and B may reflect a functional difference.

Comparison with Other Proteases. According to PDBeFold,[34] which searches for other proteins with a similar fold in the PDB, the structure of liganded 1510-N K138A is similar to that of several ClpP proteases in complexes with peptides.[35,36] ClpP catalyzes ATP-dependent protein unfolding and degradation and forms a homotetradecamer. One of the matches, *Helicobacter pylori* ClpP (HpClpP) in complex with a tetrapeptide (AAAA),[35] had a *Z* score of 7.7 with an rmsd of 2.24 Å for 145 Cα atoms, and the monomeric structure of the *E. coli* signal peptide peptidase (SppA$_{EC}$)[37] is also similar to that of liganded 1510-N K138A. SppA$_{EC}$ is one of the proteases with a Ser-Lys catalytic dyad, forms a tetrameric assembly, and

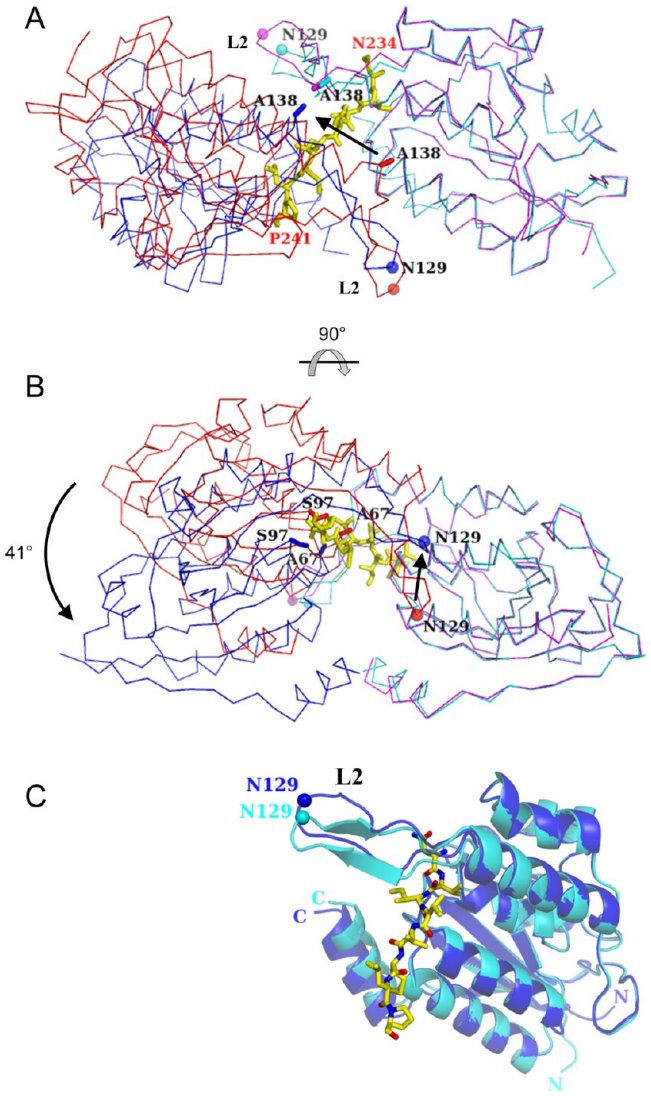

Figure 3. Superposed structures. (A) Superposed dimers of liganded and unliganded (type 2) 1510-N K138A represented in Cα traces. The view is similar to that in Figure 1A. Residues 24−120 and 139−222 of chain A of liganded 1510-N K138A are superposed with those of the unliganded form. Chain A of the liganded monomer is colored cyan and that of the unliganded monomer magenta. Chain B of the liganded form is colored blue and the other monomer of the unliganded form red. The substrate peptide is shown as yellow sticks. Side chains of Ala138 residues are also shown. The black arrow indicates the relocation (13.4 Å) of the catalytic Ala138 Cβ atom of the liganded chain B from that of the other monomer of the liganded form. The Cα atoms of Asn129, which are located at the tip of the L2 loop, are shown as spheres. (B) Side view of the superposed dimers. The liganded chain B is rotated 41° relative to the other monomer of the unliganded form. Side chains of Ala67 and Ser97 are also shown. (C) Superposition of two protomers of liganded 1510-N K138A. Residues 24−120 and 139−222 of chain B of the liganded structure are fit to those of chain A. The view is almost the same as in panel A. Chain A is shown as a cyan ribbon, and the superposed chain B is colored blue. The peptide bound to chain A is shown as sticks, and the Cα atoms of Asn129 are shown as spheres.

dx.doi.org/10.1021/bi300098k | *Biochemistry* 2012, 51, 3872−3880

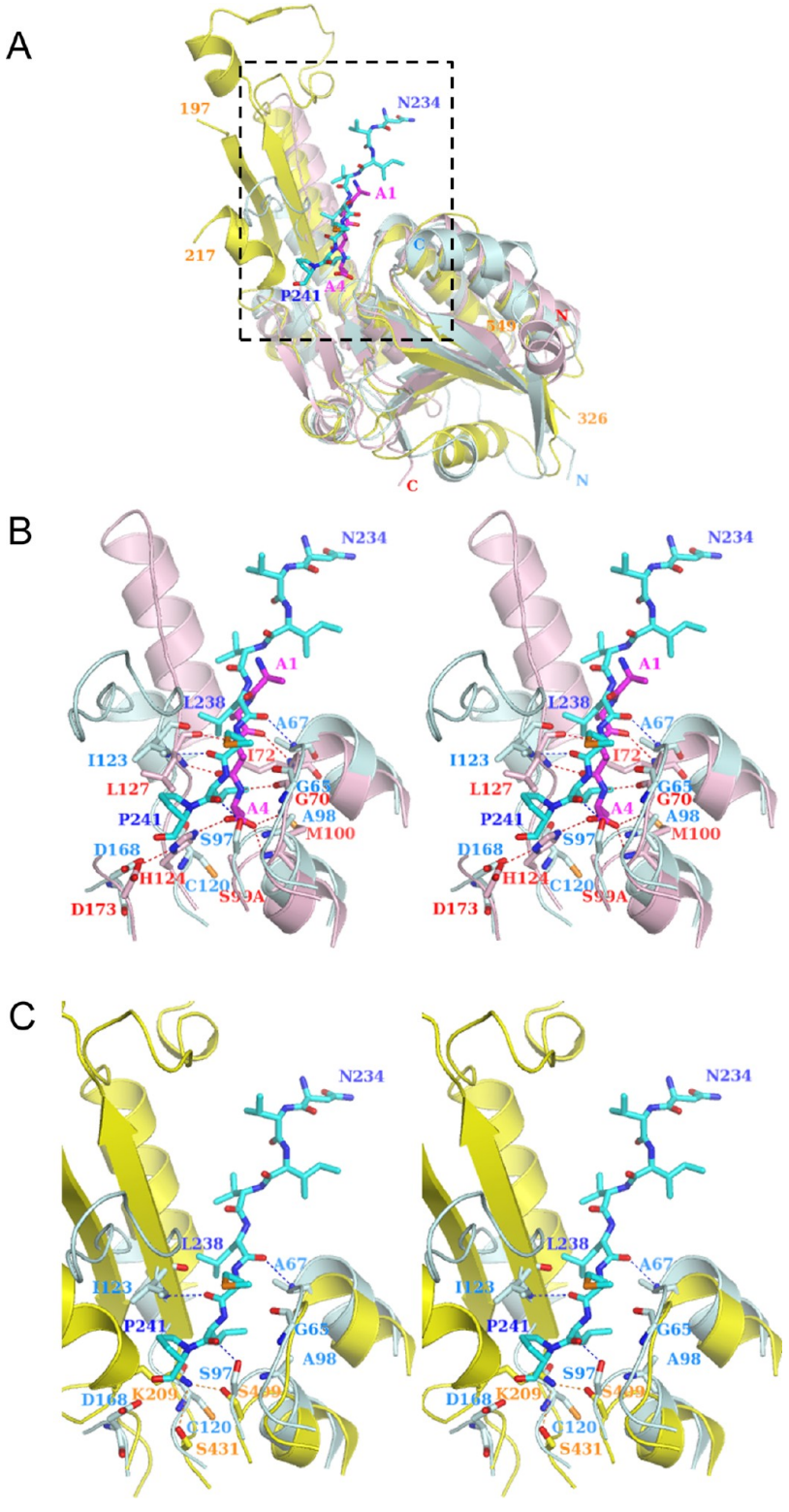

Figure 4. Structure of 1510-N K138A superposed on those of the *H. pylori* ClpP and the *E. coli* signal peptide peptidase ($SppA_{EC}$). The structure of one protomer of HpClpP in complex with the peptide AAAA (PDB entry 2zl4, chain A)[35] is superposed with that of the liganded 1510-N K138A structure (chain B), and the structure of the C-terminal half of one protomer of $SppA_{EC}$ (PDB entry 3bf0, chain C)[37] is superposed with that of the liganded 1510-N K138A structure (chain B). 1510-N K138A is represented as a cyan ribbon, and the peptide bound to 1510-N K138A is shown as cyan sticks. Some residues involved in the interaction with the peptide are represented as cyan sticks. The superposed HpClpP is shown as a pink ribbon and peptide AAAA as a magenta stick. Some residues involved in the interaction with the peptide are represented as pink sticks. The superposed $SppA_{EC}$ is shown as a yellow ribbon, and the catalytic residues are represented as yellow sticks. The residues of 1510-N K138A and the peptide are labeled in cyan and blue, respectively, those of HpClpP and the peptide in red and magenta, respectively, and those of $SppA_{EC}$ in orange. (A) Overall structures. The region shown in the dashed rectangle is magnified in panels B and C. (B) Superposition of 1510-N K138A and HpClpP in a stereoview. (C) Superposition of 1510-N K138A and $SppA_{EC}$ in a stereoview.

dx.doi.org/10.1021/bi300098k | *Biochemistry* 2012, 51, 3872−3880

cleaves the remnant signal peptides left behind in the membrane. $SppA_{EC}$ had a Z score of 8.7 with an rmsd of 2.24 Å for 165 Cα atoms. Figure 4 shows the superposition of one protomer of HpClpP and $SppA_{EC}$ with that of liganded 1510-N K138A (chain B). The overall fold is very similar except for the L2 loop corresponding to the long helix of HpClpP and $SppA_{EC}$ (Figure 4A). The catalytic Ser99 of HpClpP and the catalytic Ser409 of $SppA_{EC}$ are located at almost the same position as the catalytic Ser97 of 1510-N K138A (Figure 4B,C). HpClpP is a catalytic triad protease (Ser99, His124, and Asp173). Cys120 and Asp168 of 1510-N are located at the positions corresponding to His124 and Asp173, respectively. The C120A mutant of 1510-N shows almost the same protease activity as WT.[17] Asp168 is important for interacting with the peptide as described. In $SppA_{EC}$, one catalytic Ser409 Oγ atom is hydrogen-bonded to another catalytic Lys209 Nζ atom, and the second serine (Ser431) is also hydrogen-bonded to the Lys209 Nζ atom.[37] In 1510-N K138A, however, the catalytic lysine is not observed at the corresponding position (Figure 4C).

The SPGG motif (Ser67−Gly70) of HpClpP is located in a position similar to that of and has the same orientation as the TPGG motif (Thr62−Gly65) of 1510-N K138A. In the case of HpClpP, the oxyanion hole is formed by the amide nitrogen atoms of Gly70 and Met100.[35] Considering the structural similarity between HpClpP and 1510-N K138A, the oxyanion hole of 1510-N K138A might be formed by the amide nitrogen atoms of Gly65 and Ala98 (Figure 4B). The tetrapeptide AAAA is located in a position similar to that of the peptide of 1510-N K138A. In HpClpP in complex with the peptide, the peptide is sandwiched between two β-strands, forming a three-stranded, antiparallel β-sheet (as shown with hydrogen bonds in Figure 4B).[35] In liganded 1510-N K138A, the peptide and L1 (TPGG motif) and L2 of chain B also compose a three-stranded, antiparallel β-sheet. Although the protomers of 1510-N K138A and HpClpP are similar in structure, the L2 loop of 1510-N K138A and the long helix of HpClpP differ structurally, leading to a different form of oligomerization and a different peptide binding mode.[20]

DISCUSSION

Membrane Association. According to SOSUI,[38] PH1510p (441 residues) has one membrane-spanning region at its N-terminus (residues 7−29) and four membrane-spanning regions in its C-terminal half (residues 238−365). Thus, the following residues of 1510-N (residues 16−236) are membrane-spanning. The lower faces of the C-terminal helices of 1510-N are hydrophobic (Figure 1C), and thus, the helices would be membrane-associated. The bottom of the 1510-N dimer in Figure 1C faces the membrane located horizontally.

The 1510-N Dimer Degrades the Substrate at Only One Point. The protease activity of 1510-N is proportional not to the concentration but rather to the concentration squared of 1510-N in the concentration range of 0−0.40 μM (Figure S2 of the Supporting Information). A nonlinear dependence of protease activity on enzyme concentration is also reported for the human cytomegalovirus protease (HCMVp).[39] It is reported that the dimer of HCMVp is active whereas the monomer is inactive. According to the activity staining of 1510-N using casein-copolymerized SDS−PAGE in which protein samples were mildly denatured with sodium lauroylsarcosine instead of SDS and not heated, the 45 kDa band corresponding to the dimer shows the activity,[17] although the 25 kDa band corresponding to the monomer in the usual sample preparation does not. These results, in addition to the determined structure, suggest that two molecules of 1510-N as a dimer react with the peptide. However, the oligomeric state of full-length PH1510 (441 residues) was not determined as the full-length protein could not be expressed and purified.[17]

Using the 10-amino acid peptide ^{234}NVIVLMLPME^{243} for determination of the structure of liganded 1510-N K138A, the eight-amino acid peptide ^{234}NVIVLMLP^{241} is modeled in the structure. The catalytic Ser97 Oγ atom of chain A is hydrogen-bonded to the Asn234 O atom of the peptide, and another Ser97 Oγ atom of chain B is hydrogen-bonded to the Leu240 O atom (Figure 2A). As both catalytic Ser97 residues are located around the exit of the active tunnel, the peptide residues bound to the hydrophobic active tunnel are the central six residues ^{235}VIVLML^{240}. The pseudo-2-fold axis running between chains A and B of 1510-N K138A also runs through the peptide bond between Val237 and Leu238 of the peptide (Figure 2A). The central six residues ^{235}VIVLML^{240} are hydrophobic and in a pseudopalindromic structure as shown in Figure 2A and therefore favorably fit into the active tunnel of 1510-N.

In our previous study using the N-terminal sequences of degraded products,[17] the 1510-N protease was found to specifically cleave the hydrophobic region of the p-stomatin PH1511p between residues 238 and 239 (^{234}NVIVL↓MLPME^{243}). We again checked the cleavage site via MS of N-terminally degraded products to verify product length and the C-terminal residue (as described in the Supporting Information and Figure S3). The result indicated that 1510-N degrades at only one point between residues 238 and 239. That is, one of the two catalytic sites of the 1510-N dimer degrades the substrate at only one point. The other catalytic site does not degrade the substrate. In fact, the two protomers differ in structure quite extensively as described. Thus, the two protomers of 1510-N might have different roles (catalytic and substrate binding). However, the actual substrate of the 1510-N protease is longer, the p-stomatin PH1511p. Further structural analysis of 1510-N in complex with PH1511p is needed.

Peptide Binding Causes Large Structural Changes. The liganded structure greatly differs from the unliganded one. In the unliganded structure, the peptide-binding site and the open space beneath the site are wider as shown in Figure S4 of the Supporting Information. The rotational and translational displacement shown in Figure 3B produces a tunnel suitable for binding the peptide (Figure S4 of the Supporting Information), and therefore, the interface area between the protomers increases from 762 Å^2 (unliganded) to 951 Å^2 (liganded) as shown in Table S1 of the Supporting Information. The C-terminal helices located at the bottom (Figure 1C) also contribute to the increased interface area. If the peptide approaches from the open space beneath the peptide-binding site of 1510-N, the conformation of the dimer is changed, and salt bridges of Arg66 and Asp68 of chains A and B are formed; then the peptide-binding tunnel is produced (Figure 2C and Figure S4 of the Supporting Information).

As Figure 1A shows, the two catalytic Lys138 residues, which are replaced with Ala in the liganded 1510-N K138A dimer, are located close to each other. The distance between both Ala138 Cβ atoms of chains A and B is 3.6 Å. In unliganded 1510-N K138A, the distance between the two Ala138 Cβ atoms of the type 2 dimer is 13.6 Å (Figure 3A). These results indicate that the binding of the peptide causes a structural change that brings the two Ala138 residues of the dimer close together.

dx.doi.org/10.1021/bi300098k | Biochemistry 2012, 51, 3872−3880

Proposed Catalytic Mechanism. In both chains A and B of liganded 1510-N K138A, the catalytic Ser97 residues are relatively far from the Ala138 residues (Figure S5 of the Supporting Information). If the 1510-N WT dimer has the same structure as liganded 1510-N K138A, the side chains of Lys138 of chains A and B will produce electrostatic repulsion, and further conformational changes may occur. In the structure of the *E. coli* signal peptide peptidase, one catalytic Ser409 Oγ atom is within hydrogen bonding distance of another catalytic Lys209 Nζ atom as described previously.[37] If the close positioning of the catalytic Ser and Lys is essential for the activity of the protease with a Ser-Lys dyad, further conformational changes from the liganded 1510-N K138A structure may occur. The structure of the signal peptidase suggests that the catalytic Lys ϵ-amino group is in a deprotonated state required for its role as a general base,[19] while the optimal pH for the 1510-N activity is relatively low, 5−6,[17] indicating that the Lys138 side chain is likely to be protonated. The structure of a Lon protease from *Methanococcus jannaschii* suggests that the charged Lys side chain enters into the hydrophobic active site and assists in lowering the pK_a of the catalytic Ser hydroxyl group via its electrostatic potential.[40] 1510-N is considered to follow a mechanism similar to that of the Lon protease. The structure determined here shows the first substrate binding step of 1510-N, which is followed by a second catalytic step triggered by the conformational change of Lys138. As the cleavage site is between Leu238 and Met239 of the peptide, the catalytic Ser97 hydroxyl group attacks the Leu238 carbonyl C atom of the peptide. As shown in Figure S5 of the Supporting Information, the Ser97 Oγ atom of chain B is closer to the Leu238 C atom of the peptide (8.1 Å) than the Ser97 Oγ atom of chain A (13.8 Å). Thus, Ser97 of chain B is likely to act as a nucleophile to attack the peptide. Chain A of 1510-N tightly binds to the peptide as described, while Lys138 and Ser97 of chain B will approach the Leu238 C atom of the peptide in the second step. The structure determined here provides basic information for further functional and structural studies. To elucidate the precise function of the 1510-N protease, further structural study of the 1510-N WT or S97A mutant in complex with the peptide or a longer fragment is needed.

■ ASSOCIATED CONTENT

Supporting Information

Additional data, a supplementary table, and supplementary figures. This material is available free of charge via the Internet at http://pubs.acs.org.

Accession Codes

The atomic coordinates and structure factors have been deposited in the RCSB Protein Data Bank as entry 3VIV.

■ AUTHOR INFORMATION

Corresponding Author

*Telephone: +81-54-264-5640. Fax: +81-54-264-5641. E-mail: h-yokoya@u-shizuoka-ken.ac.jp.

Funding

This work was supported in part by a Grant-in-Aid for Young Scientists (B) (21770122) to H.Y. from the Ministry of Education, Culture, Sports, Science and Technology of Japan and also by a Sasakawa Scientific Research Grant to H.Y. from the Japan Science Society.

Notes

The authors declare no competing financial interest.

■ ACKNOWLEDGMENTS

We thank the Photon Factory staff for assistance with data collection.

■ ABBREVIATIONS

STOPP, stomatin operon partner protein; 1510-N, residues 16−236 of PH1510p; PDB, Protein Data Bank.

■ REFERENCES

(1) Arnold, I., and Langer, T. (2002) Membrane protein degradation by AAA proteases in mitochondria. *Biochim. Biophys. Acta 1592*, 89−96.

(2) Brown, M. S., Ye, J., Rawson, R. B., and Goldstein, J. L. (2000) Regulated intramembrane proteolysis: A control mechanism conserved from bacteria to humans. *Cell 100*, 391−398.

(3) Wolfe, M. S., and Kopan, R. (2004) Intramembrane proteolysis: Theme and variation. *Science 305*, 1119−1123.

(4) Tavernarakis, N., Driscoll, M., and Kyrpides, N. C. (1999) The SPFH domain: Implicated in regulating targeted protein turnover in stomatins and other membrane-associated proteins. *Trends Biochem. Sci. 24*, 425−427.

(5) Browman, D. T., Hoegg, M. B., and Robbins, S. M. (2007) The SPFH domain-containing proteins: More than lipid raft markers. *Trends Cell Biol. 17*, 394−402.

(6) Stewart, G. W., Argent, A. C., and Dash, B. C. J. (1993) Stomatin: A putative cation transport regulator in the red cell membrane. *Biochim. Biophys. Acta 1225*, 15−25.

(7) Umlauf, E., Csaszar, E., Moertelmaier, M., Schuetz, G. J., Parton, R. G., and Prohaska, R. (2004) Association of stomatin with lipid bodies. *J. Biol. Chem. 279*, 23699−23709.

(8) Umlauf, E., Mairhofer, M., and Prohaska, R. (2006) Characterization of the stomatin domain involved in homo-oligomerization and lipid raft association. *J. Biol. Chem. 281*, 23349−23356.

(9) Snyers, L., Umlauf, E., and Prohaska, R. (1998) Oligomeric nature of the integral membrane protein stomatin. *J. Biol. Chem. 273*, 17221−17226.

(10) Price, M. P., Thompson, R. J., Eshcol, J. O., Wemmie, J. A., and Benson, C. J. (2004) Stomatin modulates gating of acid-sensing ion channels. *J. Biol. Chem. 279*, 53886−53891.

(11) Wetzel, C., Hu, J., Riethmacher, D., Benckendorff, A., Harder, L, Eilers, A., Moshourab, R., Kozlenkov, A., Labuz, D., Caspani, O., Erdmann, B., Machelska, H., Heppenstall, P. A., and Lewin, G. R. (2007) A stomatin-domain protein essential for touch sensation in the mouse. *Nature 445*, 206−209.

(12) Zhang, J. Z., Hayashi, H., Ebina, Y., Prohaska, R., and Ismail-Beigi, F. (1999) Association of stomatin (band 7.2b) with Glut1 glucose transporter. *Arch. Biochem. Biophys. 372*, 173−178.

(13) Zhang, J. Z., Abbud, W., Prohaska, R., and Ismail-Beigi, F. (2001) Overexpression of stomatin depresses GLUT-1 glucose transporter activity. *Am. J. Physiol. Cell Physiol. 280*, C1277−C1283.

(14) Salzer, U., Zhu, R., Luten, M., Isobe, H., Pastushenko, V., Perkmann, T., Hinterdorfer, P., and Bosman, G. J. (2008) Vesicles generated during storage of red cells are rich in the lipid raft marker stomatin. *Transfusion 48*, 451−462.

(15) Wang, Y., Cao, D., Chen, J., Liu, A., Yu, Q., Song, X., Xiang, Z., and Lu, J. (2011) Distribution of stomatin expressing in the central nervous system and its up-regulation in cerebral cortex of rat by hypoxia. *J. Neurochem. 116*, 374−384.

(16) Green, J. B., Fricke, B., Chetty, M. C., von Düring, M., Preston, G. F., and Stewart, G. W. (2004) Eukaryotic and prokaryotic stomatins: The proteolytic link. *Blood Cells, Mol., Dis. 32*, 411−422.

(17) Yokoyama, H., and Matsui, I. (2005) A novel thermostable membrane protease forming an operon with a stomatin homolog from the hyperthermophilic archaebacterium *Pyrococcus horikoshii*. *J. Biol. Chem. 280*, 6588−6594.

(18) Paetzel, M., and Dalbey, R. E. (1997) Catalytic hydroxyl/amine dyads within serine proteases. *Trends Biochem. Sci. 22*, 28−31.

(19) Paetzel, M., Dalbey, R. E., and Strynadka, N. C. J. (1998) Crystal structure of a bacterial signal peptidase in complex with a β-lactam inhibitor. *Nature 396*, 186−190.
(20) Yokoyama, H., Matsui, E., Akiba, T., Harata, K., and Matsui, I. (2006) Molecular structure of a novel membrane protease specific for a stomatin homolog from the hyperthermophilic archaeon *Pyrococcus horikoshii*. *J. Mol. Biol. 358*, 1152−1164.
(21) Kuwahara, Y., Ohno, A., Morii, T., Yokoyama, H., Matsui, I., Tochio, H., Shirakawa, M., and Hiroaki, H. (2008) The solution structure of the C-terminal domain of NfeD reveals a novel membrane-anchored OB-fold. *Protein Sci. 17*, 1915−1924.
(22) Yokoyama, H., Fujii, S., and Matsui, I. (2008) Crystal structure of a core domain of stomatin from *Pyrococcus horikoshii* illustrates a novel trimeric and coiled-coil fold. *J. Mol. Biol. 376*, 868−878.
(23) Kuwahara, Y., Unzai, S., Nagata, T., Hiroaki, Y., Yokoyama, H., Matsui, I., Ikegami, T., Fujiyoshi, Y., and Hiroaki, H. (2009) Unusual thermal disassembly of the SPFH domain oligomer from *Pyrococcus horikoshii*. *Biophys. J. 97*, 2034−2043.
(24) Kihara, A., Akiyama, Y., and Ito, K. (1996) A protease complex in the *Escherichia coli* plasma membrane: HflKC (HflA) forms a complex with FtsH (HflB), regulating its proteolytic activity against SecY. *EMBO J. 15*, 6122−6131.
(25) Chiba, S., Ito, K., and Akiyama, Y. (2006) The *Escherichia coli* plasma membrane contains two PHB (prohibitin homology) domain protein complexes of opposite orientations. *Mol. Microbiol. 60*, 448−457.
(26) Yokoyama, H., Hamamatsu, S., Fujii, S., and Matsui, I. (2008) Novel dimer structure of a membrane-bound protease with a catalytic Ser-Lys dyad and its linkage to stomatin. *J. Synchrotron Radiat. 15*, 254−257.
(27) Otwinowski, Z., and Minor, W. (1997) Processing of X-ray diffraction data collected in oscillation mode. *Methods Enzymol. 276*, 307−326.
(28) Vagin, A., and Teplyakov, A. (1997) *MOLREP*: An automated program for molecular replacement. *J. Appl. Crystallogr. 30*, 1022−1025.
(29) Collaborative Computational Project, Number 4 (1994) The CCP4 suite: Programs for protein crystallography. *Acta Crystallogr. D50*, 760−763.
(30) Murshudov, G. N., Vagin, A. A., and Dodson, E. J. (1997) Refinement of macromolecular structures by the maximum-likelihood method. *Acta Crystallogr. D53*, 240−255.
(31) Emsley, P., and Cowtan, K. (2004) *Coot*: Model-building tools for molecular graphics. *Acta Crystallogr. D60*, 2126−2132.
(32) Winn, M. D., Isupov, M. N., and Murshudov, G. N. (2001) Use of TLS parameters to model anisotropic displacements in macromolecular refinement. *Acta Crystallogr. D57*, 122−133.
(33) Lovell, S. C., Davis, I. W., Arendall, W. B., III, de Bakker, P. I. W., Word, J. M., Prisant, M. G., Richardson, J. S., and Richardson, D. C. (2003) Structure validation by Cα geometry: φ, ψ and Cβ deviation. *Proteins: Struct., Funct., Genet. 50*, 437−450.
(34) Krissinel, E., and Henrick, K. (2004) Secondary-structure matching (SSM), a new tool for fast protein structure alignment in three dimensions. *Acta Crystallogr. D60*, 2256−2268.
(35) Kim, D. Y., and Kim, K. K. (2008) The structural basis for the activation and peptide recognition of bacterial ClpP. *J. Mol. Biol. 379*, 760−771.
(36) Szyk, A., and Maurizi, M. R. (2006) Crystal structure at 1.9 Å of *E. coli* ClpP with a peptide covalently bound at the active site. *J. Struct. Biol. 156*, 165−174.
(37) Kim, A. C., Oliver, D. C., and Paetzel, M. (2008) Crystal structure of a bacterial signal peptide peptidase. *J. Mol. Biol. 376*, 352−366.
(38) Hirokawa, T., Boon-Chieng, S., and Mitaku, S. (1998) SOSUI: Classification and secondary structure prediction system for membrane proteins. *Bioinformatics 14*, 378−379.
(39) Margosiak, S. A., Vanderpool, D. L., Sisson, W., Pinko, C., and Kan, C.-C. (1996) Dimerization of the human cytomegalovirus protease: Kinetic and biochemical characterization of the catalytic homodimer. *Biochemistry 35*, 5300−5307.
(40) Im, Y. J., Na, Y., Kang, G. B., Rho, S.-H., Kim, M.-K., Lee, J. H., Chung, C. H., and Eom, S. H. (2004) The active site of a Lon protease from *Methanococcus jannaschii* distinctly differs from the canonical catalytic dyad of Lon proteases. *J. Biol. Chem. 279*, 53451−53457.